

Analytical Determination of Slot Leakage Field and Inductances of Electric Machines with Double-Layer Windings and Semi-Closed Slots

A. Tassarolo, *IEEE, Senior Member*

Abstract—Slot leakage field and inductance computation is, in general, a non-trivial task in the analysis of electric machines equipped with semi-closed slots, even under the hypothesis of neglecting magnetic saturation. This paper proposes an analytical method to evaluate the slot leakage field and inductances in dual-layer distributed winding machines, extending the results of a previous work where the single-layer winding design was addressed. A direct solution to Poisson's differential equation in the slot domain is found by suitably defining boundary conditions in the slot opening area. Boundary conditions are defined exploiting the analytical form taken by the magnetic field in the neighborhood of ferromagnetic corner-shaped regions. The presented approach is successfully validated against Finite Element (FE) simulations.

Index Terms—Analytical methods, electric machines, leakage inductances, semi-closed slots.

I. INTRODUCTION

ALTHOUGH they are not directly involved in the electromechanical energy conversion, leakage fields and inductances need to be evaluated in the modeling and analysis of electric machines [1]-[3]. In fact, they affect machine equivalent circuit [4] and play a role in some parasitic phenomena like the occurrence of circulating currents in multiphase machines subject to inverter supply [5], [6].

A significant portion of the leakage flux is due to the magnetic field lines that cross the slots, giving rise to the so called slot leakage flux and inductances. These can be computed with simple algebraic formulas if a rectangular slot shape is used [3], [4], [6], while their computation becomes more complicated in case of a semi-closed slot design. The problem can be approached through Finite Element Analysis (FEA) [1], but analytical methods are generally preferred as a more computationally-efficient alternative, whenever possible.

The problem of analytically computing semi-closed slot leakage field and inductance has already been addressed in [7] where, however, the assumption is made that each slot includes only one coil side, as it occurs in single-layer windings. However, the vast majority of electric machines feature a dual-layer distributed winding, wherein two coil sides, generally belonging to different phases, are embedded in the same slot [8]. This paper is intended to extend the treatment proposed in [7] to the case of dual layer windings.

As done in [7], an analytical solution to Poisson's equation for the magnetic field in the semi-closed slot domain is first found and then the solution is exploited to compute the self-inductance of the coil sides in the slot as well as the mutual inductance between them. Such information is essential to compute the overall slot leakage inductance of a machine phase as explained in [3], [6]. The solution to Poisson's equation for the semi-closed slot leakage field is carried out under the hypothesis of unsaturated core and by suitably defining boundary conditions in the slot opening region. Boundary conditions are defined based on the expression taken by the magnetic vector potential in the neighborhood of right-angle ferromagnetic corner regions, which are singular points for the magnetic field [9]. This approach leads to accurately estimate the leakage flux distribution inside the semi-closed slot domain without determining the magnetic field in the entire machine [10]. The accuracy of the analytical procedure proposed is positively assessed by comparison against FEA.

The paper is organized as follows: in Section II the basic geometry of a semi-closed slot including two coil sides is described along with the modeling assumptions made for its analysis. In Section III the simplified expression of slot leakage flux and inductance is presented for subsequent comparison with the accurate one being set forth. In Section IV the magnetic leakage field inside a semi-closed slot is determined along with the inductances of the two coil sides embedded in it. Finally, in Section V some validations are proposed where the results of both the simplified and the accurate analytical model are compared to each other and to FEA simulations.

II. SEMI-CLOSED SLOT GEOMETRY AND ASSUMPTIONS

The semi-closed slot geometry being investigated in this paper is illustrated in Fig. 1. In a suitable polar coordinate system [7], the geometry is univocally defined by the four radii R_0 , R_1 , R_m , R_2 and by the angles θ_1 and θ_2 . The slot domain is subdivided into three regions, respectively denoted by letters U , V and W : regions U and V include the coil sides of the double-layer winding and are then characterized by generally non-null current densities; region W corresponds to the slot opening and is then constituted by air. We shall call I_U and I_V the total currents flowing through the coil sides respectively located in regions U and V of the slot; hence these regions will be characterized by the following current densities:

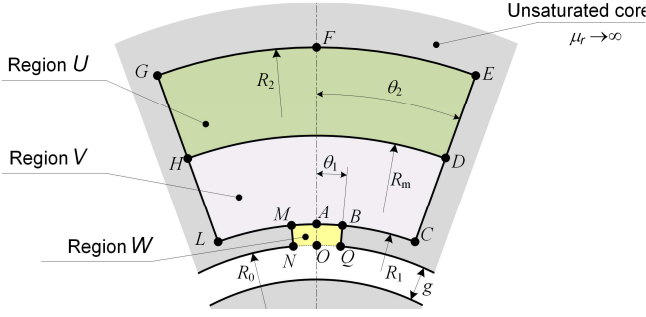


Fig. 1. Semi-closed slot geometry assumed in the paper.

$$J_U = \frac{I_U}{A_U} = \frac{I_U}{\theta_2(R_2^2 - R_m^2)}, \quad J_V = \frac{I_V}{A_V} = \frac{I_V}{\theta_2(R_m^2 - R_1^2)} \quad (1)$$

where $A_U = \theta_2(R_2^2 - R_m^2)$, $A_V = \theta_2(R_m^2 - R_1^2)$ are the cross-section areas of the regions U and V respectively.

The slot domain is supposed to be surrounded by an unsaturated ferromagnetic core, having a theoretically infinite magnetic permeability with respect to the air. This hypothesis can be restrictive for some electric machine design or operating condition, but is necessarily posed to find an analytical solution for the magnetic field in the machine domain [2], [4], [10]. Moreover, end effects are neglected in the sense that the field distribution is supposed to be the same in any cross section of the machine.

III. SIMPLIFIED MODEL FOR LEAKAGE FLUX STUDY

For the purpose of computing the slot leakage field and inductances of electric machines, approximate and simplified models have been proposed in the literature [3], [4], [6], where leakage flux lines are supposed to flow according to simple paths such as illustrated in Fig. 2. In particular, for semi-closed slots, flux lines are supposed to follow circular paths (Fig. 2b). The assumption for open rectangular slot shapes of leakage flux lines being parallel to one another and orthogonal to slot sides is quite realistic and actually leads to some simple analytical formulas that have been proved to be in good accordance with slot leakage inductances computed by FE analysis [3]. Conversely, in the case of semi-closed slots the assumption of purely circular leakage flux line paths is quite simplistic as completely disregards the significant distortions of the magnetic field near the slot opening and near slot corners.

Nevertheless, in order to have a benchmark for assessing the accuracy of the new method being set forth in this paper (Section IV), the slot leakage field formulation resulting from the simplified model (Fig. 2b) will be next derived.

A. Leakage field determination

As a first step, one needs to determine the analytical formulation of the leakage flux density in the slot domain. According to the simplified model, the flux density at any point of the slot has only a tangential component B_θ (Fig. 2b) which is supposed to be uniform along each circular flux path and thereby to depend on the polar coordinate r only.

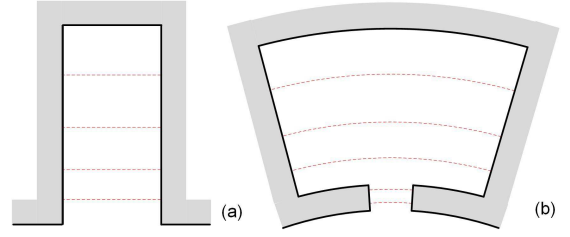


Fig. 2. Simplified leakage flux patterns (dashed lines) for (a) open rectangular slot and (b) semi-closed slot shape.

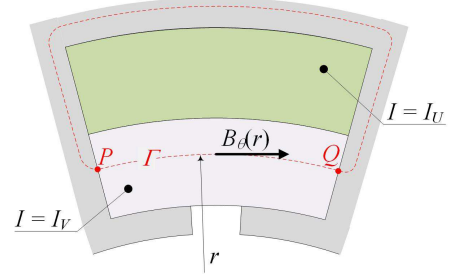


Fig. 3. Closed loop Γ for Ampere's circuital law application.

Let us consider a simplified leakage flux path Γ as shown in Fig. 3. According to the approximated model, the portion of Γ inside the slot consists of a circular arc PQ of a given radius r . Ampere's circuital law applied to Γ gives

$$B_\theta(r, I_U, I_V) = \begin{cases} \frac{\mu_0(I_U + I_V)}{2r\theta_1}, & R_0 \leq r < R_1 \\ \frac{\mu_0 I_U}{2r\theta_2} + \frac{\mu_0 I_V}{2r\theta_2} \frac{R_m^2 - r^2}{R_m^2 - R_1^2}, & R_1 \leq r < R_m \\ \frac{\mu_0 I_U}{2r\theta_2} \frac{R_2^2 - r^2}{R_2^2 - R_m^2}, & R_m \leq r \leq R_2 \end{cases} \quad (2)$$

B. Self and mutual inductance determination

Most of the algorithms available in the literature for computing slot leakage inductances of multiphase machines require the knowledge of self and mutual inductances of the individual coil sides embedded in a slot [3], [6]. More precisely, the parameters to be computed are L_U , L_V and M_{UV} where: L_U is the self-inductance of the coil side embedded in the bottom layer of the slot (region U , Fig. 1); L_V is the self-inductance of the coil side embedded in the gap-side layer of the slot (region V , Fig. 1); M_{UV} is the mutual inductance of the two coil sides embedded in the same slot. All the mentioned inductances are due to the slot leakage flux.

The values of L_U , L_V and M_{UV} can be determined based on energy considerations as follows [6]. The total magnetic energy stored in the slot leakage field can be expressed as a function of the currents I_U , I_V flowing in the two slot layers:

$$E(I_U, I_V) = \frac{L_{core}}{2\mu_0} \left[\int_{R_0-\theta_1}^{R_1} \int_{\theta_1}^{\theta_2} B_\theta(r, I_U, I_V)^2 r d\theta dr + \int_{R_1-\theta_2}^{R_2} \int_{\theta_2}^{\theta_1} B_\theta(r, I_U, I_V)^2 r d\theta dr \right], \quad (3)$$

where L_{core} is the machine core length and $B_\theta(r, I_U, I_V)$ is the flux density given by (2). At this point, the following equations can be written based on the well-known relationships between inductances and stored energy in linear systems [11]:

$$E(I, 0) = \frac{1}{2} L_U I^2, \quad E(0, I) = \frac{1}{2} L_V I^2, \quad (4)$$

$$E(I, I) = \frac{1}{2} L_U I^2 + \frac{1}{2} L_V I^2 + M_{UV} I^2,$$

where I is a generic positive current. From (4) the following expressions are derived for inductances:

$$L_U = \frac{2E(I, 0)}{I^2}, \quad L_V = \frac{2E(0, I)}{I^2}, \quad (5)$$

$$M_{UV} = \frac{E(I, I) - E(I, 0) - E(0, I)}{I^2}. \quad (6)$$

Using (2) in (3), after symbolically solving the integrals, explicit expressions can be obtained for $E(I_U, I_V)$ as follows:

$$E(I_U, I_V) = L_{core} \mu_0 \left\{ \frac{(I_U + I_V)^2 \ln(R_1/R_0)}{4\theta_1} + \frac{1}{16\theta_2} \left[I_V^2 \frac{R_m^2 + R_1^2}{R_m^2 - R_1^2} + 4f^2(I_U, I_V) \ln(R_m/R_1) - 4I_V f(I_U, I_V) \right] + \frac{I_U^2}{16\theta_2} \frac{4R_2^4 \ln(R_2/R_m) - 3R_2^4 - R_m^4 + 4R_2^2 R_m^2}{(R_2^2 - R_m^2)^2} \right\}, \quad (7)$$

where the following auxiliary function has been used:

$$f(I_U, I_V) = I_U + I_V \frac{R_m^2}{R_m^2 - R_1^2}. \quad (8)$$

The self and mutual inductances of the two coil sides can be computed by using (7) in (5) and (6). This computation method will be used, together with FE analysis, as a benchmark to assess the accuracy of the alternative model proposed in this paper and explained in the next Section.

IV. ACCURATE MODEL BASED ON SOLVING POISSON'S EQUATION

In this Section an accurate analytical model is presented to compute the slot leakage field and the inductances of a double-layer winding electric machine under the assumptions illustrated in Section II.

The method is based on solving Poisson's differential equation for the vector potential in the slot domain. The vector potential can be regarded as a scalar quantity as in any other 2D problems [7], [10]. The vector potentials will be denoted as $u(r, \theta, I_U, I_V)$, $v(r, \theta, I_U, I_V)$ and $w(r, \theta, I_U, I_V)$, respectively, in the three slot sub-domains U , V and W (Fig. 1), where r , θ are the radius and polar angle in a 2D polar coordinate system. Such functions must satisfy the following Poisson's equations:

$$\nabla u = \frac{1}{r} \frac{\partial}{\partial r} r \frac{\partial u}{\partial r} + \frac{1}{r^2} \frac{\partial^2 u}{\partial \theta^2} = -\mu_0 J_U, \quad R_m \leq r \leq R_2 \quad (9)$$

$$\nabla v = \frac{1}{r} \frac{\partial}{\partial r} r \frac{\partial v}{\partial r} + \frac{1}{r^2} \frac{\partial^2 v}{\partial \theta^2} = -\mu_0 J_V, \quad R_1 \leq r < R_m \quad (10)$$

$$\nabla w = \frac{1}{r} \frac{\partial}{\partial r} r \frac{\partial w}{\partial r} + \frac{1}{r^2} \frac{\partial^2 w}{\partial \theta^2} = 0, \quad R_0 \leq r < R_1 \quad (11)$$

A. Boundary conditions

The differential equations (9)-(11) are subject to homogenous Neumann's boundary conditions along the entire contour $QBCEGLMN$ (Fig. 1) that separates the slot domain from the surrounding ferromagnetic region. Along this contour, in fact, we have [11]:

$$\partial u / \partial n = \partial v / \partial n = \partial w / \partial n = 0 \quad (12)$$

where $\partial / \partial n$ indicates the derivative along the normal direction with respect to the boundary.

Along the arcs MB and NQ , boundary conditions cannot be exactly defined because the field on such arcs actually depends on the machine geometry outside the slot. However, it is reasonable to suppose that a sufficiently accurate prediction of the field inside the semi-closed slot is possible without the need to determine the magnetic field in the whole machine domain. In order to decouple the slot domain from the rest of the machine, the same approach used in [7] is herein adopted, assuming that the tangential flux density $B_\theta(r, \theta, I_U, I_V)$, when evaluated along arcs MB , LC and NQ (Fig. 1), can be approximated with the following functions:

$$B_\theta(R_0, \theta, I_U, I_V) = \bar{B}_\theta^{NQ}(\theta, I_U, I_V) = b_0(I_U, I_V) R_0^{-\frac{1}{3}} \left[(\theta_1 + \theta)^{-\frac{1}{3}} + (\theta_1 - \theta)^{-\frac{1}{3}} \right], \quad (13)$$

$$B_\theta(R_1, \theta, I_U, I_V) = \bar{B}_\theta^{MB}(\theta, I_U, I_V) = b_1(I_U, I_V) R_1^{-\frac{1}{3}} \left[(\theta_1 + \theta)^{-\frac{1}{3}} + (\theta_1 - \theta)^{-\frac{1}{3}} \right], \quad (14)$$

$$B_\theta(R_1, \theta, I_U, I_V) = \bar{B}_\theta^{LC}(\theta, I_U, I_V) = \begin{cases} \bar{B}_\theta^{MB}(\theta, I_U, I_V) & \text{if } -\theta_1 \leq \theta \leq \theta_1 \\ 0 & \text{if } \theta_1 \leq |\theta| \leq \theta_2 \end{cases}, \quad (15)$$

where (13)-(14) hold for $-\theta_1 \leq \theta \leq \theta_1$ and (15) for $-\theta_2 \leq \theta \leq \theta_2$ and where $b_0(I_U, I_V)$ and $b_1(I_U, I_V)$ are given by (16) as justified in the following.

$$b_0(I_U, I_V) = -\frac{\mu_0(I_U + I_V)}{3\sqrt[3]{4R_0^2\theta_1^2}}, \quad (16)$$

$$b_1(I_U, I_V) = -\frac{\mu_0(I_U + I_V)}{3\sqrt[3]{4R_1^2\theta_1^2}}.$$

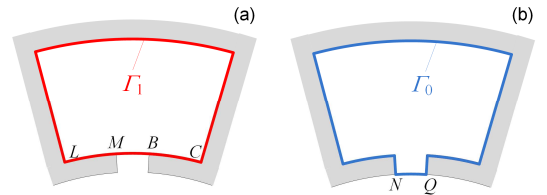


Fig. 4. Closed loops for Ampere's circuital law application.

As explained in [7], the expressions (13)-(14) are based on the observation that the magnetic field diverges as $\delta^{-1/3}$ when the distance δ from vertices M , N , B and Q tends to zero [9]. Regarding functions $b_0(I_U, I_V)$ and $b_1(I_U, I_V)$ in (16), they are derived applying Ampere's circuital law to the two closed paths Γ_0 and Γ_1 shown in Fig. 4, which yields:

$$\int_{\Gamma_0} \mathbf{B} \times d\mathbf{s} = \int_{-\theta_1}^{\theta_1} \bar{\mathbf{B}}_{\theta}^{NQ}(\theta, I_U, I_V) R_0 d\theta = \mu_0(I_U + I_V) \quad (17)$$

$$\int_{\Gamma_1} \mathbf{B} \times d\mathbf{s} = \int_{-\theta_1}^{\theta_1} \bar{\mathbf{B}}_{\theta}^{LC}(\theta, I_U, I_V) R_1 d\theta = \mu_0(I_U + I_V) \quad (18)$$

The substitution of (13)-(15) into (17)-(18) gives the expressions (16) after symbolical expansion of the integrals.

For the following it is useful to express (13)-(15) in Fourier series as follows:

$$\bar{\mathbf{B}}_{\theta}^{LC}(\theta, I_U, I_V) = \mathbf{B}_0^{LC}(I_U, I_V) + \sum_{n=1,2,\dots} \mathbf{B}_n^{LC}(I_U, I_V) \cos kn\theta, \quad (19)$$

$$\bar{\mathbf{B}}_{\theta}^{MB}(\theta, I_U, I_V) = \mathbf{B}_0^{MB}(I_U, I_V) + \sum_{n=1,2,\dots} \mathbf{B}_n^{MB}(I_U, I_V) \cosh n\theta, \quad (20)$$

$$\bar{\mathbf{B}}_{\theta}^{NQ}(\theta, I_U, I_V) = \mathbf{B}_0^{NQ}(I_U, I_V) + \sum_{n=1,2,\dots} \mathbf{B}_n^{NQ}(I_U, I_V) \cosh n\theta, \quad (21)$$

where

$$k = \pi/\theta_2, \quad h = \pi/\theta_1 \quad (22)$$

and Fourier coefficients (as functions of I_U and I_V) are:

$$\begin{aligned} \mathbf{B}_0^{MB}(I_U, I_V) &= \frac{\mu_0(I_U + I_V)}{2R_1\theta_1}, \quad \mathbf{B}_n^{MB}(I_U, I_V) = \frac{\mu_0(I_U + I_V)}{3R_1^3\sqrt{4\theta_1^5}} H_n, \\ \mathbf{B}_0^{NQ}(I_U, I_V) &= \frac{\mu_0(I_U + I_V)}{2R_0\theta_1}, \quad \mathbf{B}_n^{NQ}(I_U, I_V) = \frac{\mu_0(I_U + I_V)}{3R_0^3\sqrt{4\theta_1^5}} H_n, \quad (23) \\ \mathbf{B}_0^{LC}(I_U, I_V) &= \frac{\mu_0(I_U + I_V)}{2R_1\theta_2}, \quad \mathbf{B}_n^{LC}(I_U, I_V) = \frac{\mu_0(I_U + I_V)}{3R_1\theta_2^3\sqrt{4\theta_1^2}} K_n. \end{aligned}$$

In (23) the constants H_n and K_n are [7]:

$$K_n = \int_{-\theta_1}^{\theta_1} \cos kn\theta \left[(\theta_1 + \theta)^{-\frac{1}{3}} + (\theta_1 - \theta)^{-\frac{1}{3}} \right] d\theta \quad (24)$$

$$H_n = \int_{-\theta_1}^{\theta_1} \cosh n\theta \left[(\theta_1 + \theta)^{-\frac{1}{3}} + (\theta_1 - \theta)^{-\frac{1}{3}} \right] d\theta \quad (25)$$

These can be computed with the formulas derived in [7]:

$$K_n = \frac{2[\cos(kn\theta_1)\text{Ci}(\frac{2}{3}, 2kn\theta_1) + \sin(kn\theta_1)\text{Si}(\frac{2}{3}, 2kn\theta_1)]}{\sqrt[3]{k^2 n^2}} \quad (26)$$

$$H_n = 2[(-1)^n \text{Ci}(\frac{2}{3}, 2\pi n)] / \sqrt[3]{h^2 n^2} \quad (27)$$

where $\text{Ci}()$ and $\text{Si}()$ are the generalized cosine and sine integrals that can be defined and calculated as [12]:

$$\text{Ci}(a, z) = \int_0^z t^{a-1} \cos(t) dt = z^a \sum_{m=0}^{\infty} \frac{(-1)^m z^{2m}}{(2m+a)(2m)!} \quad (28)$$

$$\text{Si}(a, z) = \int_0^z t^{a-1} \sin(t) dt = z^a \sum_{m=0}^{\infty} \frac{(-1)^m z^{2m+1}}{(2m+a+1)(2m+1)!} \quad (29)$$

B. Analytical solution to Poisson's equation

In this Section, the analytical solution to the differential equations (9)-(11) for the vector potential in the slot domain is reported using (13)-(15) as boundary conditions to be applied in the slot opening region.

The assumed analytical expressions for the vector potentials in the three slot sub-domains U , V and W (Fig. 1) are respectively [11]:

$$\begin{aligned} u(r, \theta, I_U, I_V) &= U_{s0}(I_U) r^2 + U_{\ell 0}(I_U) \ln r \\ &+ \sum_{n=1,2,\dots} [U_n^+(I_U, I_V) r^{kn} + U_n^-(I_U, I_V) r^{-kn}] \cos kn\theta, \quad (30) \end{aligned}$$

$$\begin{aligned} v(r, \theta, I_U, I_V) &= V_{s0}(I_V) r^2 + V_{\ell 0}(I_U, I_V) \ln r \\ &+ \sum_{n=1,2,\dots} [V_n^+(I_U, I_V) r^{kn} + V_n^-(I_U, I_V) r^{-kn}] \cos kn\theta, \quad (31) \end{aligned}$$

$$\begin{aligned} w(r, \theta, I_U, I_V) &= W_{\ell 0}(I_U, I_V) \ln r \\ &+ \sum_{n=1,2,\dots} [W_n^+(I_U, I_V) r^{hn} + W_n^-(I_U, I_V) r^{-hn}] \cosh n\theta, \quad (32) \end{aligned}$$

where: (30) holds for $r \in [R_m, R_2]$ and $|\theta| \in [0, \theta_2]$; (31) holds for $r \in [R_1, R_m]$ and $|\theta| \in [0, \theta_2]$; (32) holds for $r \in [R_0, R_1]$ and $|\theta| \in [0, \theta_1]$.

The radial and tangential flux density components in the slot domain directly result from (30)-(32) as [11]:

$$\mathbf{B}_r(r, \theta, I_U, I_V) = \begin{cases} \frac{1}{r} \frac{\partial u(r, \theta, I_U, I_V)}{\partial \theta}, & r \in [R_m, R_2], |\theta| \in [0, \theta_2] \\ \frac{1}{r} \frac{\partial v(r, \theta, I_U, I_V)}{\partial \theta}, & r \in [R_1, R_m], |\theta| \in [0, \theta_2] \\ \frac{1}{r} \frac{\partial w(r, \theta, I_U, I_V)}{\partial \theta}, & r \in [R_0, R_1], |\theta| \in [0, \theta_1] \end{cases} \quad (33)$$

$$\mathbf{B}_{\theta}(r, \theta, I_U, I_V) = \begin{cases} \frac{\partial u(r, \theta, I_U, I_V)}{\partial r}, & r \in [R_m, R_2], |\theta| \in [0, \theta_2] \\ \frac{\partial v(r, \theta, I_U, I_V)}{\partial r}, & r \in [R_1, R_m], |\theta| \in [0, \theta_2] \\ \frac{\partial w(r, \theta, I_U, I_V)}{\partial r}, & r \in [R_0, R_1], |\theta| \in [0, \theta_1] \end{cases} \quad (34)$$

In the expression for the scalar potential $w(r, \theta, I_U, I_V)$ in (32) the term proportional to r^2 is omitted because such potential must satisfy Laplace's differential equation (11); the same term is, instead, included in potentials $u(r, \theta, I_U, I_V)$ and $v(r, \theta, I_U, I_V)$ so as to account for the non-null current-density forcing terms in Poisson's equations (9)-(10).

The trigonometric expansions in (30)-(32) are chosen so as to automatically satisfy homogenous Neumann's boundary conditions on slot sides, i.e. on segments QB , CE , LG and NM (Fig. 1). In fact, according to (33) it can be seen that the radial flux density is identically null on such segments, i.e.:

$$B_r(r, \theta_2, I_U, I_V) = B_r(r, -\theta_2, I_U, I_V) = 0, \quad R_1 \leq r \leq R_2 \quad (35)$$

$$B_r(r, \theta_1, I_U, I_V) = B_r(r, -\theta_1, I_U, I_V) = 0, \quad R_0 \leq r \leq R_1 \quad (36)$$

In the assumed expressions for the scalar potential (30)-(32) there appear some unknown functions of I_U and/or I_V , which need to be determined by imposing that (9)-(11) must be satisfied together with the following conditions (Fig. 1):

- homogeneous Neumann's boundary condition on GE ;
- continuity condition for the radial flux density component across HD ;
- continuity condition for the tangential flux density component across HD ;
- non-homogeneous boundary condition on arc LC , i.e. the tangential flux density on LC must be equal to (15);
- non-homogeneous boundary condition on arc NQ , i.e. the tangential flux density on NQ must be equal to (13).

By direct substitution of (30)-(32) into (9)-(11) one can immediately find that, for the latter to be satisfied, functions $U_{s0}(I_U)$ and $V_{s0}(I_V)$ must be equal to:

$$U_{s0}(I_U) = -\frac{\mu_0 I_U}{4\theta_2(R_2^2 - R_m^2)}, \quad V_{s0}(I_V) = -\frac{\mu_0 I_V}{4\theta_2(R_m^2 - R_1^2)}. \quad (37)$$

Then, imposing the boundary conditions listed above leads to determine the other unknowns in (30)-(32) as:

$$U_{\ell 0}(I_U) = -2R_2^2 U_{s0}(I_U),$$

$$V_{\ell 0}(I_U, I_V) = 2R_m^2 [U_{s0}(I_U) - V_{s0}(I_V)] - 2R_2^2 U_{s0}(I_U),$$

$$W_{\ell 0}(I_U, I_V) = \mu_0 (I_U + I_V) / (2\theta_1),$$

$$U_n^+(I_U, I_V) = V_n^+(I_U, I_V) = \frac{R_1^{kn+1} B_n^{LC}(I_U, I_V)}{kn(R_1^{2kn} - R_2^{2kn})}$$

$$U_n^-(I_U, I_V) = V_n^-(I_U, I_V) = \frac{R_1^{kn+1} R_2^{2kn} B_n^{LC}(I_U, I_V)}{kn(R_1^{2kn} - R_2^{2kn})},$$

$$W_n^+(I_U, I_V) = \frac{R_0^{hn+1} B_n^{NQ}(I_U, I_V) - R_1^{hn+1} B_n^{MB}(I_U, I_V)}{hn(R_0^{2hn} - R_1^{2hn})},$$

$$W_n^-(I_U, I_V) = \frac{R_0^{hn+1} R_1^{2hn} B_n^{NQ}(I_U, I_V) - R_1^{hn+1} R_0^{2hn} B_n^{MB}(I_U, I_V)}{hn(R_0^{2hn} - R_1^{2hn})}. \quad (38)$$

C. Computation of slot leakage inductances

The knowledge of functions (37) and (38) enables one to fully determine the vector potential in the slot domain through (30)-(32) and the flux density by means of (33)-(34). Once the flux density is known, the magnetic energy stored in the slot leakage field can be determined as [11]:

$$E(I_U, I_V) =$$

$$\frac{L_{core}}{2\mu_0} \left\{ \int_{R_0-\theta_1}^{R_1} \int_{\theta_1}^{\theta_2} [B_r(r, \theta, I_U, I_V)^2 + B_\theta(r, \theta, I_U, I_V)^2] r d\theta dr \right. \\ \left. + \int_{R_1-\theta_2}^{R_2} \int_{\theta_2}^{\theta_1} [B_r(r, \theta, I_U, I_V)^2 + B_\theta(r, \theta, I_U, I_V)^2] r d\theta dr \right\} \quad (39)$$

The analytical formulation of the flux density components B_r , B_θ found in the previous subsection makes it possible to solve (39) symbolically. This leads to express the energy stored in the slot as shown in (40) at the bottom of the page.

At this point, based on the same reasoning made in Section III.B for the simplified model, the relationships (4) can be written and, from them, the self-inductances of the two coil sides (L_U , L_V) as well as their mutual inductance (M_{UV}) can be obtained through (5)-(6) in which the accurate expression (40) for $E(I_U, I_V)$ is used.

V. VALIDATIONS BY COMPARISON WITH FEA

In this Section, the results obtained for the slot leakage field and inductance computation by direct solution of Poisson's equation (Section IV) are assessed by comparison with FEA calculations. Furthermore, the same results are compared to the prediction made through the simplified model described in Section III in order to evaluate the extent to which the new proposed model enhances the accuracy of the estimation.

For the purpose of FEA validations, the geometric model shown in Fig. 5 is considered. The model is characterized by the dimensions given in Table I.

TABLE I. CHARACTERISTIC DIMENSIONS OF THE MODEL CONSIDERED FOR FEA SIMULATIONS

R_0	140 mm	R_m	175 mm	θ_1	2.711°	L_{core}	100 mm
R_1	150 mm	R_2	200 mm	θ_2	11.53°	g	10 mm

$$E(I_U, I_V) = \frac{L_{core}}{\mu_0} \left\{ \theta_2 \left[U_{\ell 0}^2(I_U) \ln\left(\frac{R_2}{R_m}\right) + (R_2^4 - R_m^4) U_{s0}^2(I_U) + 2(R_2^2 - R_m^2) U_{s0}(I_U) U_{\ell 0}(I_U) \right] \right. \\ \left. + \theta_2 \left[V_{\ell 0}^2(I_U, I_V) \ln\left(\frac{R_m}{R_1}\right) + (R_m^4 - R_1^4) V_{s0}^2(I_V) + 2(R_m^2 - R_1^2) V_{s0}(I_V) V_{\ell 0}(I_U, I_V) \right] \right. \\ \left. + \theta_1 W_{\ell 0}^2(I_U, I_V) \ln\left(\frac{R_1}{R_0}\right) + \frac{\pi}{2} \sum_{n=1,2,\dots} n \left[U_n^{+2}(I_U, I_V) (R_2^{2kn} - R_1^{2kn}) - U_n^{-2}(I_U, I_V) (R_2^{-2kn} - R_1^{-2kn}) \right] \right. \\ \left. + \frac{\pi}{2} \sum_{n=1,2,\dots} n \left[W_n^{+2}(I_U, I_V) (R_1^{2hn} - R_0^{2hn}) - W_n^{-2}(I_U, I_V) (R_1^{-2hn} - R_0^{-2hn}) \right] \right\} \quad (40)$$

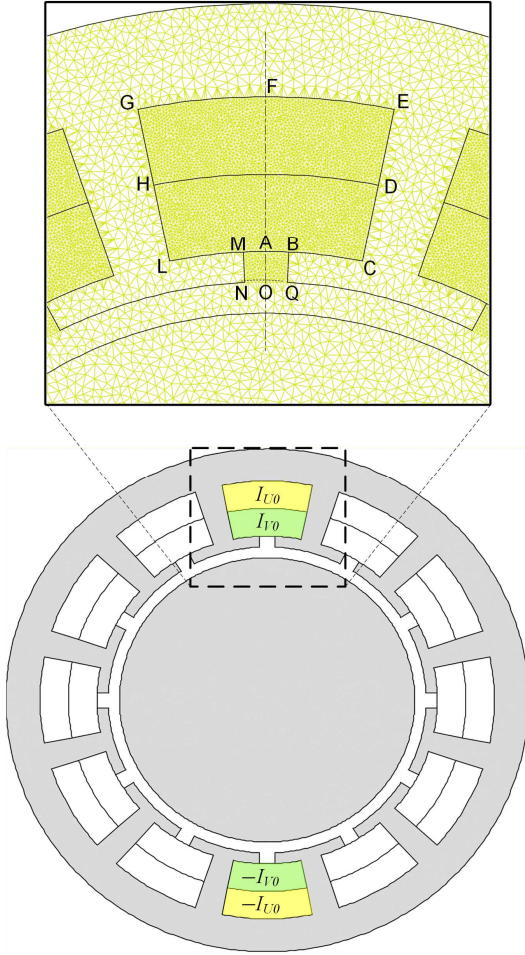


Fig. 5. Slot model (with relevant mesh) used for slot field simulation through FEA.

The meaning of the symbols appearing in Table I is illustrated in Fig. 1.

As to the gap width g , it is initially set at $g=10$ mm, but simulations are run for different values of g to assess the extent to which the analytical solution found in the slot domain is actually independent of the machine geometry outside the slot.

The assessment of the proposed method by comparison with FEA is first addressed looking at the predicted flux density in the slot domain. For this purpose, coil side currents are assigned the example values below.

$$I_U = I_{U0} = 5000 \text{ A}, \quad I_V = I_{V0} = -2500 \text{ A} \quad (41)$$

In the model shown in Fig. 5, the focus is on the magnetic field inside the upper (zoomed) slot energized with currents I_{U0} and I_{V0} ; however, as shown in Fig. 5, another slot, displaced by the 180° and energized with opposite currents $-I_{U0}$ and $-I_{V0}$, is considered so that the total current flowing through the model cross section is zero.

The flux density values resulting from the field solution presented in Section IV.B are compared to those obtained from FEA along some significant contours of the slot domain. Examples of such comparison are shown in Fig. 6

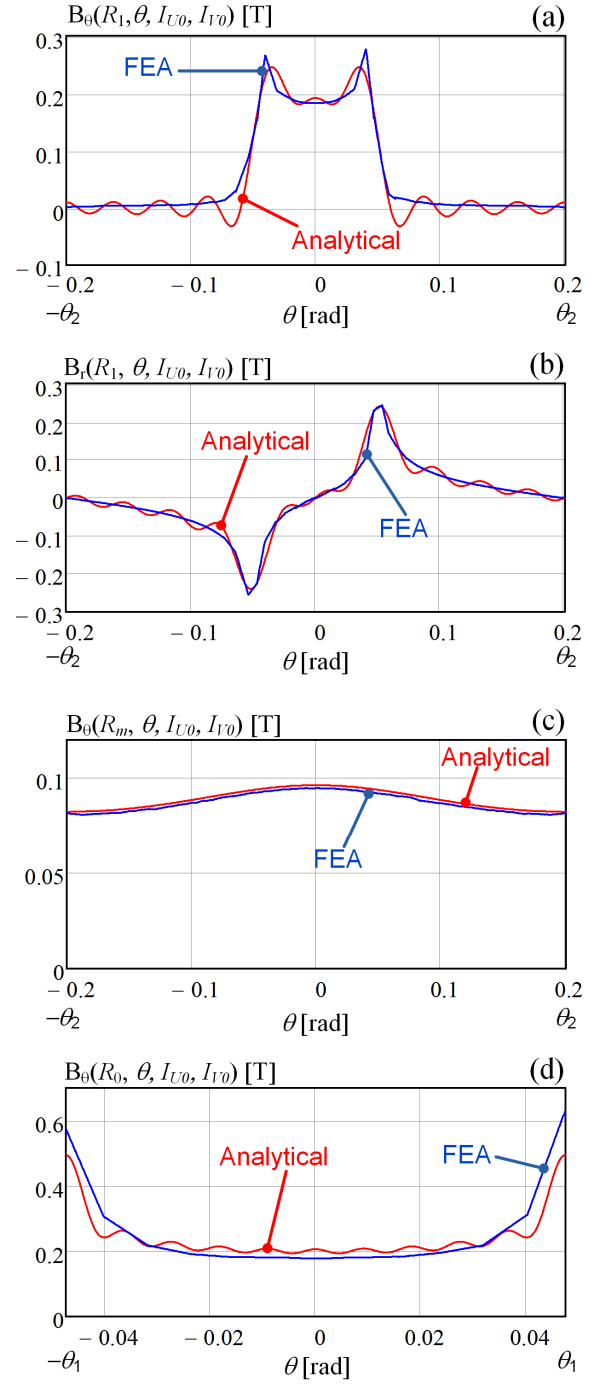


Fig. 6. Flux density components computed analytically and by FEA along significant model contours for coil side currents $I_{U0} = 5000$ A and $I_{V0} = -2500$ A: (a) tangential flux density on arc LC; (b) radial flux density on arc LC; (c) radial flux density on arc HD; (d) tangential flux density on arc NQ.

and Fig. 7 proving that the proposed approach is capable of predicting the slot leakage flux density in the slot with a satisfactory accuracy.

It is noted that, in Fig. 6 and Fig. 7, the accurate model is used considering the first ten harmonics; in other words, the index n appearing in all Fourier series expansions derived in Section IV ranges from 1 to 10.

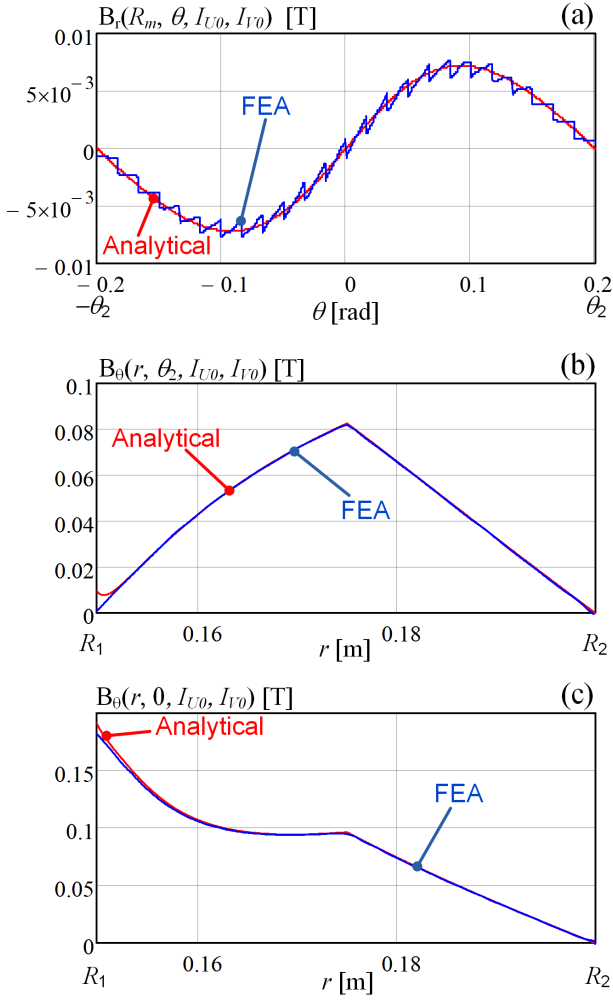


Fig. 7. Flux density components computed analytically and by FEA along significant model contours for coil side currents $I_{U0} = 5000$ A and $I_{V0} = -2500$ A: (a) radial flux density on arc HD ; (b) tangential flux density on segment CE ; (c) tangential flux density on segment AF .

As a further check, the self and mutual inductances L_U, L_V, M_{UV} of the coil sides embedded in the slot are evaluated based on (5)-(6) where the energy $E(I_U, I_V)$ stored in the slot is independently evaluated both with the simplified model (Section III.B) and with the proposed accurate one (Section IV.C). In the latter case, the first ten harmonics of Fourier series expansions ($n=1,2,\dots,10$) are again considered. The comparison is repeated for different values of the gap g , while the slot geometry is maintained the same as shown in Fig. 5 with the other dimensions given in Table I. The results are illustrated in Fig. 8 and Fig. 9.

From Fig. 8 and Fig. 9 the following remarks can be drawn:

- The proposed accurate analytical model (Section IV) gives an estimation of self and mutual inductance that very well matches the same quantities computed by FEA, with errors below 3%.
- Conversely, the simplified analytical model (Section III) appears to be very inaccurate, leading to overestimate inductances by 20-30% with respect to FEA results.

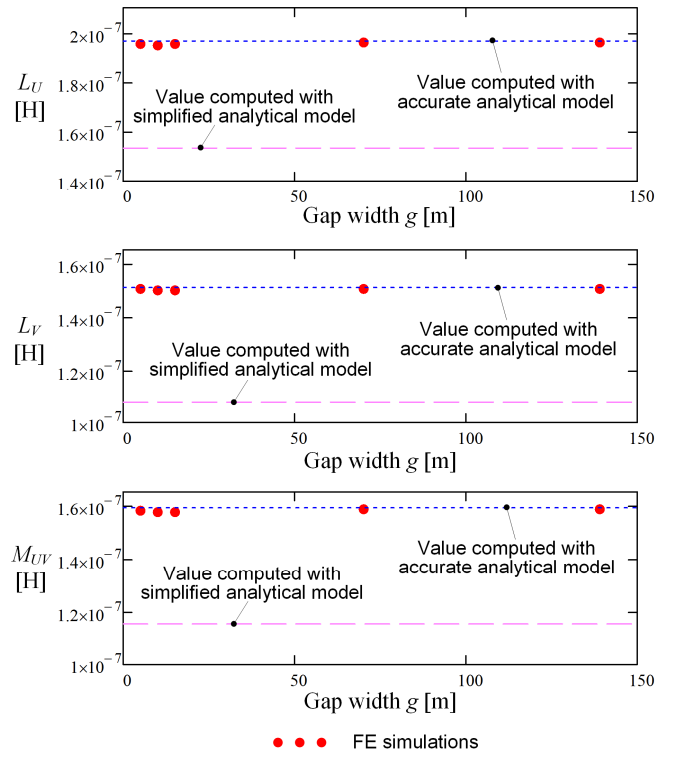


Fig. 8. Self and mutual inductances of slot coil sides independently computed in three different ways.

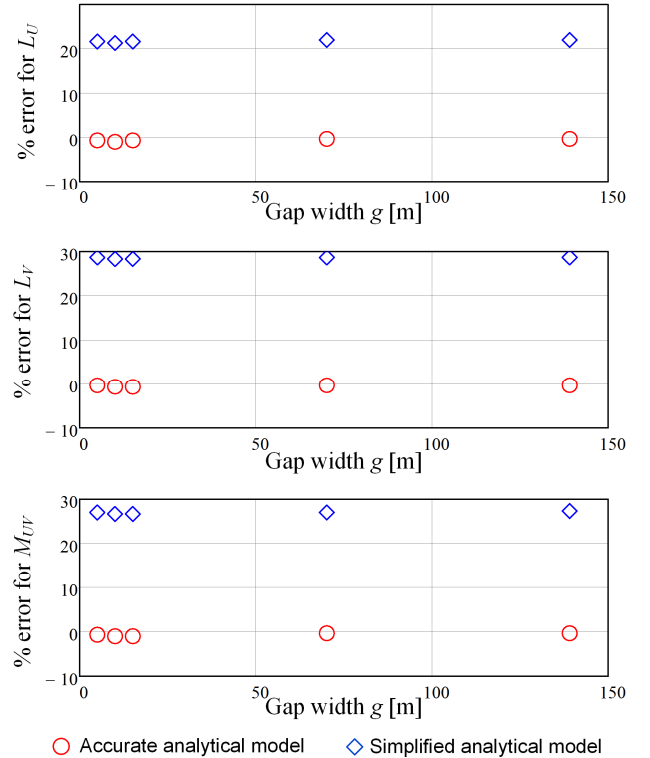


Fig. 9. Percent error (with respect to FEA results) of inductance estimation through the simplified and accurate analytical approach.

- The error of the accurate analytical method with respect to FEA, although in any case acceptable, exhibits some dependency on the gap width. In

particular, the analytical prediction given by the proposed model appears to be the asymptotical approximation of FEA result when the air gap g tends to infinity. In other words, analytically computed values practically coincide with FEA estimations for very large gaps (corresponding to the physical situation where the rotor of the electric machine is withdrawn). This was already observed in [7].

The last remark has a quite intuitive physical interpretation. In fact, the accurate analytical model is based on assuming that the tangential flux density in the slot opening region can be approximated by (13)-(15), wherein rotor effects are disregarded. Such an approximation is precise for relatively large gap values, while it becomes slightly less precise when the gap decreases and the rotor presence tends to affect the flux density values in the slot opening area. The errors introduced, however, can be seen to be definitely acceptable.

A final note is about the effect of magnetic saturation. In this respect, it needs to be observed that all the treatment proposed in this paper assumes an infinitely-permeable core, which leads to the so-called “unsaturated” values of slot leakage inductances. In [7] it is shown how magnetic saturation causes slot leakage inductances to decrease with respect to their unsaturated values. The same observations made in [7] for single-layer windings obviously hold for the dual-layer winding design addressed in this paper, too. Also in this case, it can be said that an accurate estimation of leakage inductances in presence of significant magnetic saturation generally requires the use of FEA.

VI. CONCLUSION

In this paper an accurate analytical method has been presented to determine the slot leakage field and inductances for electric machines with semi-closed slots and double-layer distributed windings. The analytical formulations obtained are an extension of those presented in a previous work for the case of single-layer windings. The approach adopted in the paper is based on directly solving Poisson’s differential equation for the vector potential in the semi-closed slot domain. An analytical field solution for the slot leakage flux has been determined in the paper by suitably defining boundary conditions on the slot opening region. For this purpose, the specific mathematical form taken by the flux density in the neighborhood of right-angle ferromagnetic corners (which are singular point for the magnetic field) has been exploited. Such boundary condition setting has led to decouple the slot domain from the rest of the machine geometry, making it possible to determine the leakage flux distribution inside the slot without knowing the field outside it. The analytical technique proposed in the paper has been validated against FE simulations and shown to give very accurate results, with errors less than 5%. Conversely, the application of alternative simplified models, frequently adopted in the literature, are shown to give poor accuracy, with errors ranging between 20% and 30% with respect to FEA simulations.

In conclusion, the methodology presented is deemed to be a convenient and efficient alternative to time-consuming

FEA, at least for those machine designs and operating conditions that allow for magnetic saturation effects to be neglected.

VII. REFERENCES

- [1] K. Shima, K. Ide, M. Takahashi, “Analysis of leakage flux distributions in a salient-pole synchronous machine using finite elements”, *IEEE Transactions on Energy Conversion*, vol. 18, no. 1, pp. 63-70, Mar 2003.
- [2] D. Ban, D. Zarko, I. Mandic, “Turbogenerator end-winding leakage inductance calculation using a 3-D analytical approach based on the solution of Neumann Integrals”, *IEEE Transactions on Energy Conversion*, vol. 20, no. 1, pp. 98-105, March 2005.
- [3] A. Tassarolo, D. Giulivo, “Analytical methods for the accurate computation of stator leakage inductances in multi-phase synchronous machines”, *2010 International Symposium on Power Electronics Electrical Drives Automation and Motion (SPEEDAM)*, pp. 845-852, 14-16 June 2010.
- [4] A. Boglietti, A. Cavagnino, M. Lazzari, “Computational Algorithms for Induction-Motor Equivalent Circuit Parameter Determination—Part I: Resistances and Leakage Reactances”, *IEEE Transactions on Industrial Electronics*, vol. 58, no. 9, pp. 3723-3733, Sept. 2011.
- [5] A. Tassarolo, C. Bassi, “Stator harmonic currents in VSI-fed synchronous motors with multiple three-phase armature windings”, *IEEE Transactions on Energy Conversion*, vol. 25, no. 4, Dec. 2010, pp. 974-982.
- [6] D. Hadiouche, H. Razik, A. Rezzoug, “On the modeling and design of dual-stator windings to minimize circulating harmonic currents for VSI-fed AC machines”, *IEEE Transactions on Industry Applications*, vol. 40, Mar./Apr. 2004, pp. 506-515.
- [7] A. Tassarolo, “Leakage Field Analytical Computation in Semi-Closed Slots of Unsaturated Electric Machines”, *IEEE Transactions on Energy Conversion*, in press. Early access available through IEEEExplore.
- [8] P. Krause, O. Wasynczuk, S. Sudhoff, S. Pekarek, *Analysis of Electric Machinery and Drive Systems*, Wiley, 2013.
- [9] Z.C. Li, T.T. Lu, “Singularities and treatments of elliptic boundary value problems”, *Mathematical and Computer Modelling*, vol. 31, no. 8-9, Apr.-May 2000, pp. 97-145.
- [10] A. Rahideh, T. Korakianitis, “Analytical Magnetic Field Calculation of Slotted Brushless Permanent-Magnet Machines With Surface Inset Magnets”, *IEEE Transactions on Magnetics*, vol. 48, no. 10, pp. 2633-2649, Oct. 2012.
- [11] J. D. Jackson, *Classical Electrodynamics*, John Wiley and Sons, New York, 1999.
- [12] M. Abramowitz and I. A. Stegun, “Sine and Cosine Integrals”, in *Handbook of Mathematical Functions with Formulas, Graphs, and Mathematical Tables*, Dover, 1972, pp. 231-233.



Alberto Tassarolo (M’06—SM’15) received his Laurea and Ph.D. Degrees in Electrical Engineering from the University of Trieste, Italy, in 2000 and from the University of Padova, Italy, in 2011, respectively. Until 2006, he worked in the design and development of innovative motors and generators for high power applications with NIDEC-ASI (formerly Ansaldo Sistemi Industriali). Presently, he is with the Engineering and Architecture Department of the University of Trieste, Italy, where he teaches the course of Electric Machine Design. His main research interests are in the area of electric machine and drive modeling, design and analysis, a field in which he has authored more than 100 scientific papers. He acts as the principal investigator for various research projects in cooperation with leading electric machine manufacturers and final users, including the Italian Navy. He serves as an Editor for the *IEEE TRANSACTIONS ON ENERGY CONVERSION* and as an Associate Editor for the *IEEE TRANSACTIONS ON INDUSTRY APPLICATIONS*. He is a registered professional engineer in Italy.